

Master thesis
Electrical Engineering
September 2018.



Master Thesis
In Electrical Engineering with
Emphasis on Signal Processing
September 2018

Identification and Masking Method of Clouds in Satellite Images

Emani Harsha Yashaskar

Department of Applied Signal Processing
Blekinge Institute of Technology
SE-371 79 Karlskrona, Sweden

This thesis is submitted to the Department of Applied Signal Processing at Blekinge Institute of technology in partial fulfilment of the requirements for the degree of Master of Science in Electrical Engineering with Emphasis on Signal Processing.

Contact Information:

Author:

EMANI HARSHA YASHASKAR

E-mail: haem17@student.bth.se

Supervisor:

Irina Gertsovich

Industrial reference:

Supervisor

Dr. K.Venugopal Rao, NRSC/ISRO.

University Examiner:

Dr. Sven Johansson

Department of Applied Signal Processing
Blekinge Institute of Technology
SE-371 79 Karlskrona, Sweden

Internet : www.bth.se
Phone : +46 455 38 50 00
Fax : +46 455 38 50 57

Acknowledgements

I would first like to thank my thesis advisor Irina Gertsovich of Department of Applied Signal Processing, Blekinge Institute of Technology for everything she has done to me. I would like to thank her for guiding me from Sweden and steered me in the right direction whenever she thought I needed it. Her cooperation in the thesis was immense and would be never forgotten and she was always available whenever I needed the help of her.

I would also like to thank my thesis advisor Dr. K Venugopal Rao Group Head (Urban studies/GIS) at NRSC for proving me a chance to work at ISRO-NRSC Hyderabad. His office was always open whenever I ran into a trouble spot or had a question about my research or writing. He was also cooperative through out the thesis work. I would also like to take the opportunity to thank all the members of NRSC Urban studies group for their support during this master thesis work.

I would also like to thank Sven Johansson from my university, who has been very kind to me throughout this thesis work.

Finally, I thank and express my profound gratitude to my parents and to all my friends for providing me with unfailing support and continuous encouragement throughout my years of study and through the process of researching and writing this thesis. This accomplishment would not have been possible without them. Thank you everyone.

Emani Harsha Yashaskar

ABSTRACT

Identification of the cloud in an image is essential in order to remove the noise in the image and improve the quality of the image. Further the masking of cloud in a satellite image is important in order to obtain a clear image taken from a remote sensing satellite. This thesis presents the identification of cloud in a satellite image, to segregate the cloud part of the image from non-cloud part of the same image like soil, vegetation, water by using certain techniques. Region of interest (ROI) selection technique is used to obtain the desired cloud image from the actual image. To obtain cloud image from non-cloud image masking methods such as automatic masking and manual masking are used in ROI selection technique. A suitable image is obtained from the sensor known as 'Moderate Resolution Imaging Spectroradiometer' (MODIS). The manual and automatic masked cloud images are compared and the performance of the cloud masking methods is evaluated. The evaluation of the results indicates that the cloud images are possible to be obtained by ROI selection technique through automatic masking and manual cloud masking method.

Key words: Automatic masking method, Cloud, Manual masking method, MODIS sensor, Region of interest (ROI) selection technique.

Table of Contents

List of figures	7
List of tables	9
1 INTRODUCTION	10
1.1 Remote sensing	10
1.2 Information about sensors and QGIS software	11
1.2.1 LISS-I	11
Thematic mapper Landsat-8	14
MODIS	14
1.2.2 QGIS software	15
1.3 ROI selection technique and masking methods	15
1.3.1 Masking methods	15
1.4 Problem Statement	16
1.5 Research questions	17
2 LITERATURE STUDY	18
3 BACKGROUND	20
3.1 Why MODIS sensor?	20
3.2 Why QGIS?	24
4 METHODOLOGY	26
4.1 Selection of suitable sensor	27
4.2 Selection of an image	27
4.3 QGIS Application	28
4.4 Analysing techniques and Application of Region of Interest (ROI)	29
4.5 Masking methods	30
4.5.1 Otsu method of thresholding	30
4.5.2 Binarization using threshold	30
4.6 Comparison of the results of manual and automatic maskings	31
5 RESULTS AND DISCUSSIONS	33
5.1 Cloud separation from non-cloud	33
5.2 Manual masking method	34
5.2.1 Freehand manual masking of cloud	34
5.2.2 Manual masking of cloud by threshold varying	38
5.3 Automatic masking method	41

5.4 Comparison and analysis of manual masking and automatic masking methods	42
5.5 Discussions	44
6 CONCLUSION AND FUTURE WORK	46
6.1 Conclusions	46
6.2 Future works	46
6.3 Challenges	47
References	48

List of figures

<i>Figure 1-1 . IRS-1A [7]</i>	11
<i>Figure 1-2. LISS-I sensor</i>	12
<i>Figure 1-3. Resourcesat-1</i>	13
<i>Figure 1-4. AWIFS-1 sensor</i>	13
<i>Figure 1-5. HDF image obtained from MODIS sensor</i>	16
<i>Figure 3-1. MODIS sensor[21]</i>	20
<i>Figure 3-2. MODIS sensor subsystems[22]</i>	21
<i>Figure 3-3. MODIS sensor components[6]</i>	21
<i>Figure 4-1. overview of implementation project</i>	26
<i>Figure 4-2. HDF image obtained from MODIS sensor</i>	27
<i>Figure 4-3. Processed image from QGIS</i>	28
<i>Figure 5-1. Graph showing the maximum values of the cloud and non-cloud regions across spectral bands</i>	33
<i>Figure 5-2. Graph showing the minimum values of the cloud and non-cloud regions across spectral bands:</i>	34
<i>Figure 5-3. Freehand masking of cloud</i>	35
<i>Figure 5-4. Masked patch of cloud</i>	35
<i>Figure 5-5. Actual cloud image</i>	36
<i>Figure 5-6. Image with cloud of the freehand masking method</i>	36
<i>Figure 5-7. Freehand masking of cloud</i>	37
<i>Figure 5-8. Masked patch of cloud</i>	37
<i>Figure 5-9. Image with cloud of the freehand masking method</i>	38
<i>Figure 5-10. Original greyscale image</i>	39
<i>Figure 5-11. Cloud image using manual masking method with threshold level=10</i>	39
<i>Figure 5-12. Cloud image using manual masking method with threshold level=129</i>	40
<i>Figure 5-13. Cloud image using manual masking method with threshold level=250</i>	40
<i>Figure 5-14. Original greyscale image</i>	41
<i>Figure 5-15. Cloud image using automatic masking method with threshold level=0.5059</i>	42
<i>Figure 5-16. Graph showing manual threshold=10 and the pixel difference between automatic masking & manual masking=4058</i>	43

Figure 5-17. Graph showing manual threshold=250 and the pixel difference between automatic masking & manual masking=1385 43

Figure 5-18. Graph showing manual threshold=129 and the pixel difference between automatic masking & manual masking=0 44

List of tables

<i>Table 1.1. Specifications of LISS-I sensor[4]</i>	12
<i>Table 1.2. AWIFS-1 features[4]</i>	14
<i>Table 1.3. MODIS sensor dimensions[8]</i>	14
<i>Table 3.1. Specifications of MODIS sensor[8]</i>	22
<i>Table 3.2. MODIS sensor bands [8]</i>	22
<i>Table 4.1. Maximum and minimum data recorded from the image in QGIS</i>	29

1 INTRODUCTION

1.1 Remote sensing

Remote sensing is the science and art of acquisition of data about an object, or phenomenon with making no physical contact with the object or area which is under study [1]. Remote sensing is considered to be the conducive factor to science by observing data through various kinds of images day by day. In order to employ remote sensing, we have our own eyes as an example which act as sensors corresponding to the light which gets reflected from the current page. Our eyes obtain the “data” as impulses which refers to the amount of light that gets reflected from the dark and light areas on the page [1].

In modern era, the term “remote sensing” corresponds to the use of satellite based sensor technologies, which is used to detect and classify the objects on earth which includes on the surface, in the atmosphere and oceans. These satellites remotely sense the data located on the earth surface, atmosphere and oceans [2].

Using various satellites and sensors we remotely collect the data that can be analysed to obtain the information about the objects, areas, or phenomena being investigated[1]. Some of the examples of satellites are RESOURCESAT-1, RESOURCESAT-2, Indian remote sensing (IRS) satellites etc which are used to obtain images for scientific and other various purposes.

In recent years, remote sensing is playing a crucial role in location and utilization of earth resources. This is done by employing electromagnetic energy sensors that are being operated from airborne and spaceborne platforms which assist in mapping and monitoring of earth resources.

The earth resources consists of various fields like soil, vegetation, and water at surface level. Each field behaves differently in various bands of electromagnetic (EM) spectrum. Clouds are visible at atmospheric level and these clouds are no exception for behaviour in EM spectrum. The mapping and monitoring of the different fields are done by satellites with suitable sensors on board [3].

1.2 Information about sensors and QGIS software

As discussed in section 1.1 about various types of satellites, there are various sensors contained in these satellites which are used for obtaining images. They are:

- Linear imaging self scanning (LISS)-1 sensor [4].
- Advanced wide field sensor (AWIFS)-1 [4].
- Thematic mapper Landsat-8 [5].
- Moderate resolution imaging spectroradiometer (MODIS) [6].

1.2.1 LISS-I

Linear imaging self scanning (LISS)-I is a kind sensor which is seen in a satellites such as IRS-1A, IRS-1B. This sensor is used to obtain images with different resolution, swath width and sensor channels such as LISS-I-1, LISS-I-2, LISS-I-3, LISS-I-4. The images taken from the satellites stated above are obtained by employing this sensor and these satellite images exhibit spectral limits for various spectral bands within the resolution [4].

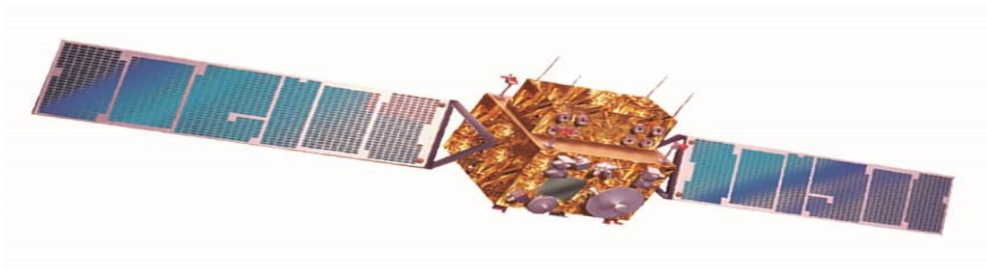


Figure 1-1 . IRS-1A [7]

Figure 1.1 depicts the Indian remote sensing satellite (IRS)-1A.

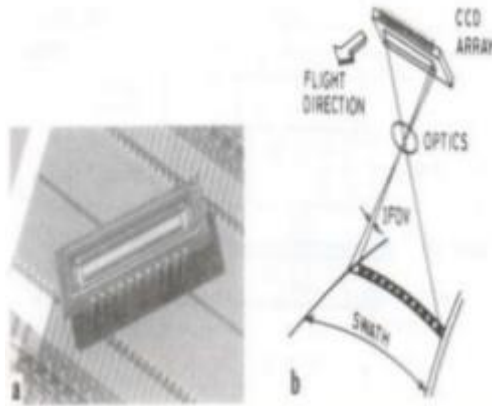


Figure 1-2. LISS-I sensor

Some of the important features of LISS-1 are shown in Table 1.1.

Table 1.1. Specifications of LISS-I sensor[4]

Sensor	Resolution (metres)	Swath width (km)	Sensor channels
LISS-I	72	148	LISS-I-1 LISS-I-2 LISS-I-3 LISS-I-4

AWIFS-1

Advanced wide field sensor (AWIFS)-1 is a kind of sensor used in various satellites such as RESOURCESAT-1, RESOURCESAT-2, IRS satellites [4]. The AWIFS-1 sensor is used to obtain images of variations in resolution, and swath width. The images obtained from the satellites are through this sensor having spectral limits for respective spectral bands within the resolution [4].

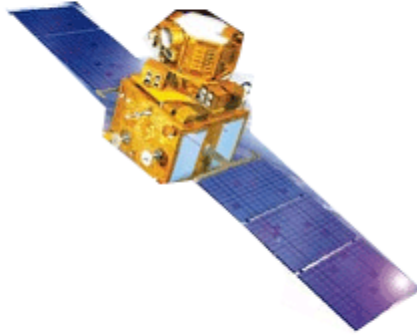


Figure 1-3. Resourcesat-1

Figure 1.3 shows the resourcesat-1 satellite used in remote sensing.



Figure 1-4. AWIFS-1 sensor

Figure 1.4 shows the advanced wide field (AWIFS)-1 sensor. Some of the important features of AWIFS-1 are shown in Table 1.2.

Table 1.2. AWIFS-1 features[4]

Sensor	Resolution (metres)	Swath width (km)	Sensor channels
AWIFS-1	56-70	370-740	AWIFS-1 AWIFS-2 AWIFS-3 AWIFS-4

Thematic mapper Landsat-8

It is a kind of sensor used in American satellites has Operational land imager (OLI) and Thermal infrared sensor (TIRS) providing moderate-resolution imagery and operates in the visible, near-infrared, short wave infrared, and thermal infrared spectrums. It is an enhancement of previous landsat-4, landsat-5 and landsat-7 sensors. It consists of 9 spectral bands [5].

MODIS

Moderate resolution imaging spectroradiometer (MODIS) is a sensor which is operated by Terra (EOS AM) and Aqua (EOS PM) satellites. It is a payload imaging sensor. It is operated in 36 spectral bands useful to track the changes in landscape over times. And also used to detect changes in earth's cloud cover, oceans etc. It is a key instrument in earth observing system (EOS) satellites. The 36 spectral bands are in visible region, near-infrared region, thermal infrared region.

Some of the important features of MODIS are shown in Table 1.3

Table 1.3. MODIS sensor dimensions[8]

Size	1.0 x 1.6 x 1.0 m
Weight	228.7 kg
Power	162.5 W
Spatial resolution	250m (bands1-2), 500m (bands3-7), 1000m (bands8-36)

1.2.2 QGIS software

Quantum geographic information system (QGIS) is a software which allows users to view, analyse, and edit the geospatial data [9]. In addition, it is used to compose and export the graphical maps. QGIS has two layers; they are: raster and vector layers.

The point, line, or polygon features of the maps or data are stored as vector data. This QGIS offers various methods to modify the data or the map image. By having an image one can modify or obtain desired images from the actual image in QGIS. For example: one can increase or decrease the contrast, brightness, and make other various adjustments in the image using QGIS [9].

1.3 ROI selection technique and masking methods

Region of interest (ROI) are the samples which are identified for a particular purpose within a dataset [10]. This ROI concept is applied in many areas, for example, in geographical information systems (GIS) a ROI is taken as a polygonal, circular, elliptical, and also free hand selection from a given 2-dimensional map [10]. Also used in medical imaging in defining the boundaries of a tumour or any image related to this field [10]. The ROI defines the borders of an object which is under consideration in computer vision and optical character recognition [10].

The ROI is a portion of an image that can be analysed or can be modified by other operations such as filtering. In this work ROI is used in operation to create binary mask image, where the pixels that belong to ROI are set to 1 and the pixels outside ROI are set to 0. More than one ROI can be selected in an image [11].

1.3.1 Masking methods

Masking of cloud is a prerequisite in order to map the land surface attributes [12]. The satellite image of land surface to be obtained contains cloud cover and is considered to be a noise, so identification and masking of clouds is an important task to achieve the desired satellite image [13].

The masking method is one of the methods involved in ROI selection technique. The masking methods may involve automatic masking and manual masking.

1.4 Problem Statement

MODIS sensor is used in satellites to obtain images of various spectral bands and various spectral resolutions. The images provided by MODIS are used for various purposes such as detecting changes in earth's surfaces vegetation, soil, water. While obtaining the image of the earth from the satellite, there is a chance for occurrence of cloud in the image, as satellites take the picture of land surface from the space. So, the cloud here is considered as a noise in the image. There is a need for identifying or recognition of the cloud and masking it, in order to obtain the desired image.



Figure 1-5. HDF image obtained from MODIS sensor

Figure 1.5 shows the HDF (Hierarchical Data Format) image obtained from the MODIS sensor.

- Cloud identification and masking of cloud of the image obtained from MODIS sensor is main motive for the project.
- Study of different techniques and methods used to identify and mask the cloud for obtaining the desired image.

1.5 Research questions

- What type of technique is required to approach to mask the Tagged Image File Format (TIFF) image obtained from the satellite?
- What methods are involved in the technique to obtain the desired cloud ROI in the image?

2 LITERATURE STUDY

The studies of identification of cloud by masking method is conducted in several surveys. The methodologies used for the cloud recognition are different in different surveys. The cloud identification is done through a remote sensing satellite using various sensors such as LISS-I, AWIFS, and MODIS sensor is employed in various studies and papers. Cloud recognition is considered as the important process before removing the cloud. The wide range of spectral bands offered by the MODIS sensor are used for the cloud identification of an image. For the identification of cloud and the separation of it from the non-cloud images the other methods were adopted such as homomorphic filter method, bag of words method, template synthesis method, et al.

Xiaoning Song, Zhenhua Liu, Yingshi Zhao presented a paper on the recognition of cloud. The identification of cloud in this paper is by using MODIS sensor. In this paper the method is the multi-spectral synthesis method adopted to distinguish the cloud and land surface and the other method is automatic cloud detection algorithm in which the cloud pixels are determined by thresholds and these thresholds are determined by man-machine interaction using neural networks [14].

In the paper presented by Yi Yuan, Xiangyun Hu, the study shows that the automatic cloud detection is done based on the bag-of-words (BOW) model. The experiment shows that the precision of cloud extraction is high when compared to the other methods [15].

Fei Liu, Cheng-Fan Li, Jing-yuan Yin conducted a study on extraction of cloud for remote sensing (RS) image by combining various methods. The methods employed in this technique were principal component analysis (PCA), independent component analysis (ICA), and support vector machine (SVM) algorithms. The image obtained for cloud identification was from the MODIS sensor. The cloud extraction is done from the vast area of volcanic ash [16].

In the paper presented by Warinthorn Kiadtikornthaweeoyot the cloud image is obtained from the Landsat satellite. The paper presents the problem of cloud cover as a major obstacle for land surface analysis. This paper presents the assessment of cloud cover using ROI selection technique but based on image classification and histogram segmentation for THAICHOTE satellite

images. A detailed study to accurately determine the percentage of cloud cover is done in this paper [17].

Byambasuren Bat-Erdene conducted a study on using the automatic region of interest (ROI) in image processing [18].

Daniel Di Rosa, Claudia Notarnicola, Francesco Posa presented a paper on validation of cloud masking of MODIS aqua image by cross comparison method [19].

Lin Sun, Xueting Mi, Jing Wei, Jian Wang, Xinoeng Tian, Huiyong Yu, Ping Gan presented a paper on cloud detection algorithm for remote sensing data at visible to short-wave infrared wavelengths. This paper proposes an automatic cloud detection algorithm for multispectral remote sensing sensors which demonstrates an accurate detection rate of more than 85% [20].

3 BACKGROUND

3.1 Why MODIS sensor?

The Moderate Resolution Imaging Spectroradiometer (MODIS) is a payload imaging sensor launched by National Aeronautics and Space Administration (NASA) in 1999.

As discussed in earlier section that MODIS sensor offers images with a wide range of spectral bands and wavelengths ranging between $0.4\mu\text{m}$ - $14.4\mu\text{m}$ in electromagnetic (EM) spectrum and spatial resolution of 250m, 500m, and 1km is offered by MODIS sensor.

Further this MODIS sensor is operated by Terra (EOS AM) and Aqua (EOS PM) satellites. The 36 spectral bands of MODIS are in visible region, near-infrared region, thermal infrared region. Terra's orbit around the earth is timed in such a way that it passes from north to south across the equator in the morning, while Aqua orbits around the earth from south to north over the equator in the afternoon. Terra MODIS and Aqua MODIS will view the entire earth's surface every 1 to 2 days by acquiring the data in 36 spectral bands or groups of wavelengths. This data is helpful to understand the global dynamics and changing processes occurring on the land, in the oceans, and in the lower surface of the atmosphere [6].

In the development of validated, global, interactive earth systems MODIS plays a vital role to predict the changes occurring globally.

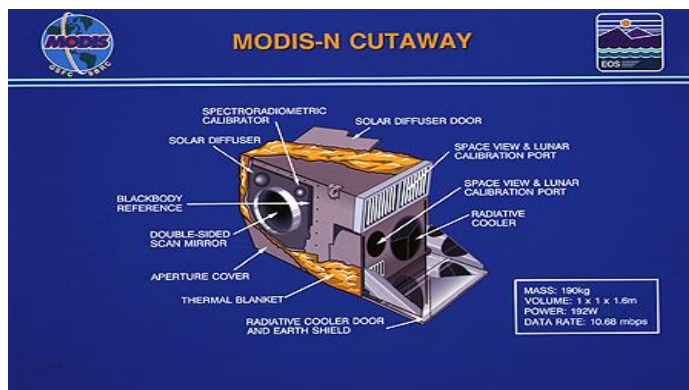


Figure 3-1. MODIS sensor[21]

Figure 3.1 depicts the information about various parts used in constructing MODIS sensor.

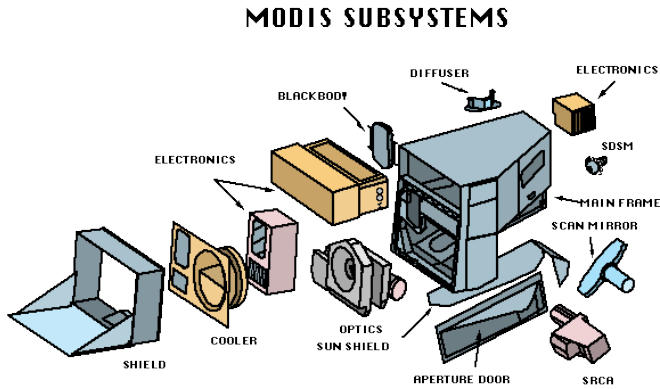


Figure 3-2. MODIS sensor subsystems[22]

MODIS sensor subsystems which contain the diffuser, electronics, optics sunshields, shields, apertures, frames, and mirrors are shown in Figure 3.2.

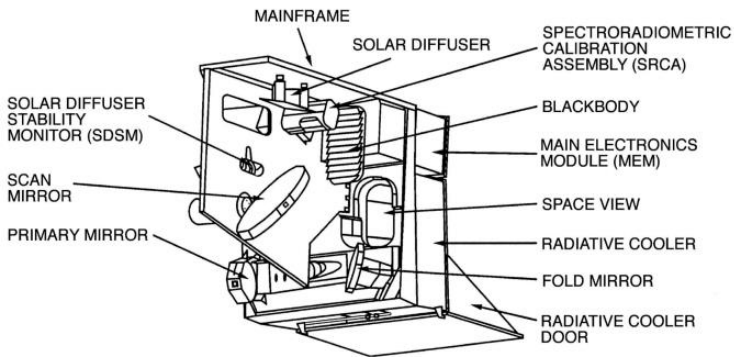


Figure 3-3. MODIS sensor components[6]

Figure 3.3 shows a detailed picture of the MODIS sensor's components.

Specifications of MODIS:

Table 3.1. Specifications of MODIS sensor[8]

Orbit	705km, 10:30 am. Descending node (terra) or 1:30 pm. Ascending node (aqua), sun synchronous, circular
Scan rate	20.3 rpm, cross track
Swath	2330 km (cross track)

MODIS bands:

Table 3.2. MODIS sensor bands [8]

Band	Wavelength (nm)	Resolution (m)	Primary use
1	620-670	250	Land/cloud/aerosols boundaries
2	841-876	250	Land/cloud/aerosols boundaries
3	459-479	500	Ocean colour/phytoplankton/biogeochemistry
4	545-565	500	Ocean colour/phytoplankton/biogeochemistry
5	1230-1250	500	Ocean colour/phytoplankton/biogeochemistry
6	1628-1652	500	Ocean colour/phytoplankton/biogeochemistry
7	2105-2155	500	Ocean colour/phytoplankton/biogeochemistry
8	405-420	1000	Ocean colour/phytoplankton/biogeochemistry
9	438-448	1000	Ocean colour/phytoplankton/biogeochemistry
10	483-493	1000	Ocean colour/phytoplankton/biogeochemistry

11	526-536	1000	Ocean colour/phytoplankton/biogeochemistry
12	546-556	1000	Ocean colour/phytoplankton/biogeochemistry
13	662-672	1000	Ocean colour/phytoplankton/biogeochemistry
14	673-683	1000	Ocean colour/phytoplankton/biogeochemistry
15	743-753	1000	Ocean colour/phytoplankton/biogeochemistry
16	862-877	1000	Ocean colour/phytoplankton/biogeochemistry
17	890-920	1000	Atmospheric water vapour
18	931-941	1000	Atmospheric water vapour
19	915-965	1000	Atmospheric water vapour
Band	Wavelength (µm)	Resolution (m)	Primary use
20	3.660-3.840	1000	Surface/cloud temperature
21	3.929-3.989	1000	Surface/cloud temperature
22	3.929-3.989	1000	Surface/cloud temperature
23	4.020-4.080	1000	Surface/cloud temperature
24	4.433-4.498	1000	Atmospheric temperature
25	4.482-4.549	1000	Atmospheric temperature
26	1.360-1.390	1000	Cirrus clouds water vapour
27	6.535-6.895	1000	Cirrus clouds water vapour
28	7.175-7.475	1000	Cirrus clouds water vapour
29	8.400-8.700	1000	Cloud properties
30	9.580-9.880	1000	Ozone

31	10.780- 11.280	1000	Surface/cloud temperature
32	11.770- 12.270	1000	Surface/cloud temperature
33	13.185- 13.485	1000	Cloud top altitude
34	13.485- 13.785	1000	Cloud top altitude
35	13.785- 14.085	1000	Cloud top altitude
36	14.085- 14.385	1000	Cloud top altitude

In order to obtain the cloud image of various bands and spectral characteristics the MODIS sensor is very much useful. The cloud's size, location, shape and areas in the visible region, infrared red region images are obtained through this sensor from the respective satellite. The texture, brightness of a cloud image depends on the sun's illumination, reflectivity (cloud thickness), relative positions of cloud, sun, and radiometer [6].

On an infrared (IR) picture, the brightness of cloud image depends upon the temperature of emitting surface i.e. the brighter the image, the colder (higher) the cloud top. IR is obtained in EM spectrum, where atmosphere is nearly transparent, so the radiation from clouds and surface reach satellite relatively unaffected by atmosphere. MODIS sensor is also helpful to detect the position of moving clouds and its geographical position is also seen as clouds move with wind.

3.2 Why QGIS?

As discussed in the section 3.1, Quantum geographic information system (QGIS) is a software application which can be freely modified to perform specialize or more different tasks. It is an application that supports editing, analysis, and viewing of geospatial data i.e. the data or image taken from a satellite from space. The image obtained from the satellite need to be

processed by various methods in order to obtain the desired image. So, the satellite image is processed into QGIS to increase or decrease the contrast, brightness, and various adjustments in the image. This is done by the layers of QGIS, they are: vector layer and raster layer. The point, line, or polygon features of the maps or data are stores as vector data [9].

The raster layer data is made up of pixels also referred as grid cells. In this layer the images can be stored in different formats, for example: Geo TIFF (Geographic Tagged Image File Format), JPEG (Joint Photographic Experts Group), ECW (Enhanced compression Wavelet), HDF (Hierarchical Data Format), etc [9].

In addition to this QGIS, ERDAS (Earth Resources Data Analysis Systems) Imagine which is also an image processing software. QGIS is mostly preferred to obtain the desired image.

4 METHODOLOGY

A flowchart displaying complete overview of the work performed in this thesis is shown in Figure 4.1.

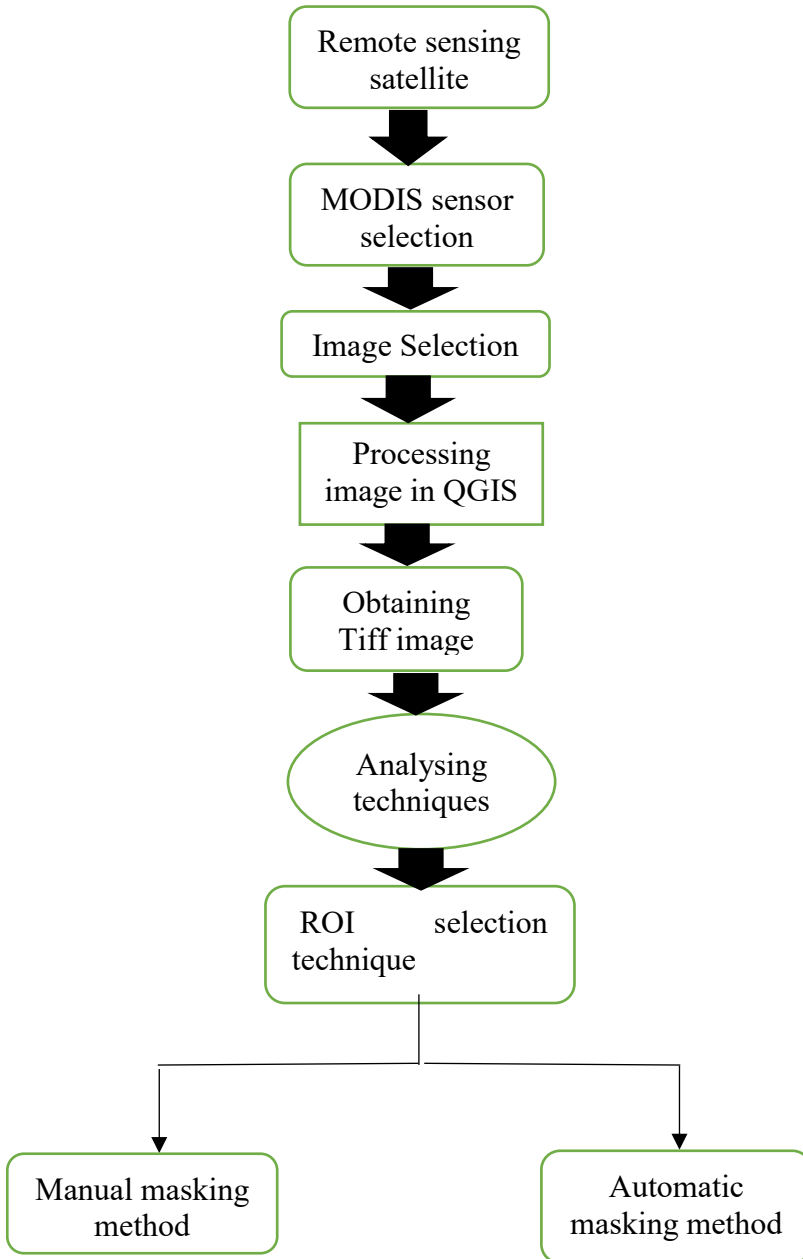


Figure 4-1. overview of implementation project

4.1 Selection of suitable sensor

The remote sensing satellites in space function with different sensors to capture images of the earth and atmosphere. Various sensors of the satellites have been discussed earlier. Out of all MODIS sensor offers various facilities to capture the desired images and the MODIS sensor is selected to capture the image.

4.2 Selection of an image

A suitable image is selected from the MODIS sensor to carry out the process of cloud identification. In order to obtain the suitable image MODIS sensor offers wider range of spectral bands and characteristics. The image which is contained with the clouds is selected. The MODIS image obtained is in HDF (Hierarchical Data Format) image which is to be converted into TIFF (Tagged Image File Format) image in QGIS.



Figure 4-2. HDF image obtained from MODIS sensor

Figure 4.2 shows the HDF (Hierarchical Data Format) image obtained from the MODIS sensor.

4.3 QGIS Application

The processing of image in QGIS is very important in order to obtain the desired image. The image obtained from the MODIS sensor is made to process in the QGIS software to obtain the image show as below. The image shown below is adjusted in contrast, brightness, and saturation to get the desired image. Further the data is recorded from the image. The data is recorded from the cloud, vegetation, water, land. This process of recording data of four various kinds is done to obtain the cloud data separated from non-cloud data (vegetation, water, land). The data recorded is used to obtain graphs of cloud and compared with non-cloud part in the graph.

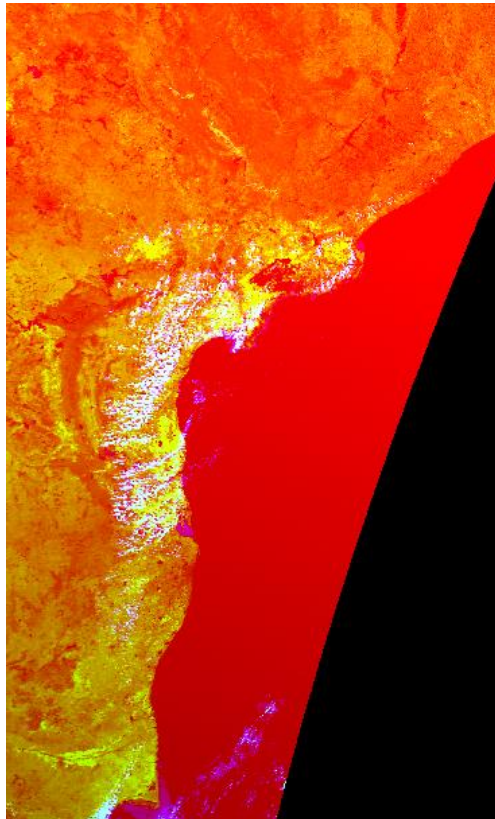


Figure 4-3. Processed image from QGIS

Figure 4.3 shows the TIFF (Tagged Image File Format) image of QGIS.

Table 4.1. Maximum and minimum data recorded from the image in QGIS

Maximum values	Band 1	Band 2	Band 3	Band 4	Band 5	Band 6	Band 7
Cloud	3481	7431	6935	7538	7560	6300	4544
Vegetation	3533	2119	3147	917	2497	2246	1611
Water	3495	1782	1131	1329	1845	1545	1110
Land	3689	3767	658	1115	3537	3408	2331
Minimum values	Band 1	Band 2	Band 3	Band 4	Band 5	Band 6	Band 7
Cloud	3269	2844	1218	1356	3088	2318	1431
Vegetation	3398	1608	218	409	2015	147	540
Water	3478	348	533	875	327	213	167
Land	3529	2446	191	543	2564	1561	676

Table 4.1 shows the maximum and minimum values of cloud and non-cloud fields of various bands of ‘nm’ units.

4.4 Analysing techniques and Application of Region of Interest (ROI)

Region of interest (ROI) is considered to be an important technique used to mask the TIFF image to obtain the desired image i.e. the cloud image. Other than ROI, there are techniques to identify and mask the cloud, they are: Support vector machine (SVM) method, Bag of words method etc. The selection of region of interest technique is done with the help of MATLAB. Here the original image is converted in to a greyscale image with the help of MATLAB. Hence in the ROI technique, masks are created for the original image and then masking methods are done further to obtain the desired image.

4.5 Masking methods

Masking methods are considered to be the integral part of the ROI selection technique. The masking methods that are used in this thesis are the manual masking method and automatic masking method.

In manual masking the greyscale image is converted into binary image by selecting the region of interest manually. The part of the image containing the cloud which is obtained, is assumed to be the desired cloud image. The part of image containing cloud is further compared to the cloud image obtained from the automatic masking.

In automatic masking the greyscale image is converted into the binary image automatically by the algorithm. The part of image containing the cloud of the automatic part is then compared to the part of image containing the cloud image which is obtained manually. Hence the images containing the cloud of both the methods are compared and analysed such that both the images obtained are same in identifying the cloud.

4.5.1 Otsu method of thresholding

The Otsu method is an algorithm used to calculate the image thresholding performed automatically. In simple words, the Otsu's method is implemented by reduction of a grey level image to a binary image performed in MATLAB. The desired cloud image is obtained automatically by this thresholding using equation (4.1). Thresholding is considered as an important technique for image processing. Here in this method, the algorithm assumes two classes of pixels (foreground pixels and background pixels) of an image. Then the optimum threshold level is calculated by minimizing intra-class variance by using equation (4.1) :

$$\sigma_w^2(t) = \omega_0(t)\sigma_0^2(t) + \omega_1(t)\sigma_1^2(t) \quad (4.1)$$

Weights ω_0 and ω_1 are the probabilities of the two classes of pixels separated by a threshold t , and σ_0^2 and σ_1^2 are variances of these two classes of pixels [23].

4.5.2 Binarization using threshold

The binarization of image is done by thresholding. The simplest property that pixels can share in a region is intensity. In order to segment those regions the method used is thresholding, which is separation of light and dark regions.

Thresholding creates binary images from converting grey-level pixels below some threshold to zero and all the pixels above that threshold to one [25].

The image I is downsampled into 305x556 elements of greyscale image, therefore the procedure of manual classification of pixels as cloud or non-cloud takes shorter time.

If $e(x,y)$ is a pixel in a binary image, based on $u(x,y)$ at some global threshold T ,

$$e(x,y) = \begin{cases} 1, & \text{if } u(x,y) \geq T \\ 0, & \text{otherwise} \end{cases} \quad (4.2)$$

4.6 Comparison of the results of manual and automatic maskings

In order to evaluate the difference between the two masked cloud images i.e. manual masked and automatic masked cloud, subtraction is done for both masks to obtain the desired cloud image. The binary images using automatic and manual methods are created to obtain the desired image. In the manual method and automatic method the values of pixels are set such that for a given value of 'I', the image obtained has cloud part if the part of image I is equal to 1 and else it is equal to 0. For different pixel values of 'I' the image containing cloud obtained through the manual method are compared to the image obtained in the automatic method. This process is done until the pixel value difference between the images of both the methods is equal to zero. The desired image is obtained when the pixel difference between images of both methods is equal to zero.

For example: let the greyscale image 'I' containing the cloud obtained by manual method is denoted by P and let the greyscale image containing the cloud obtained by automatic method be denoted by Q. Now 'P' binary mask, denoted by BW is obtained by applying a threshold value T to P, according to the equation 4.2. The binary mask of 'Q' is denoted by BW_{auto} and is obtained by the threshold value T set by the Otsu' method for the automatic masking method according to equation 4.2.

Given two matrices P and Q, both which are of size N x M, the difference Q-P is N x M matrix whose entries are formed by subtracting entries of Q from corresponding entries of P. If $R=Q-P$, then $R_{ij}=Q_{ij}-P_{ij}$.

Therefore matrix 'R' will contain the differences between corresponding entries in matrices BW and BWauto. The total number 'k' of different entries in R can be found according to the equation (4.3).

$$k = \sum_{i=1}^N \sum_{j=1}^M |R_{ij}|, \quad (4.3)$$

where N and M are the number of rows and columns in the binary masks BW and BWauto.

For threshold $T = 10$, the number of different pixels i.e. $k = 4058$.

For threshold $T = 100$ the pixel difference $k = 1116$, and the k values are calculated for $T = 20, 30, 40, \dots, 250$ pixel values. Here in this case the pixel difference i.e. $k = 0$ when $T = 129$. Hence the cloud image is obtained at this $T = 129$ i.e. where the pixel difference is zero.

5 RESULTS AND DISCUSSIONS

5.1 Cloud separation from non-cloud

The image containing the cloud and the non-cloud are separated and the graphs of maximum values and minimum values at different wavelengths and bands are plotted with respect to the cloud and the non-cloud fields (vegetation, water, land) as shown in Figure 5.1 and Figure 5.2. The data recorded from the TIFF image of the cloud and the non-cloud areas are represented in different spectral bands.

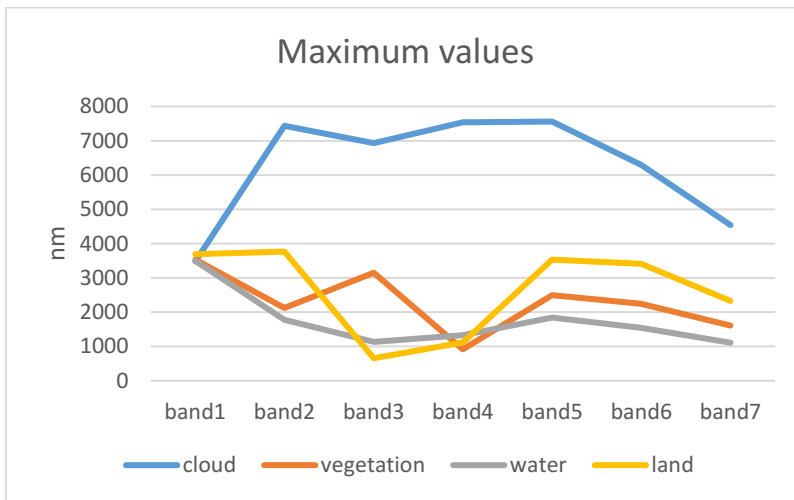


Figure 5-1. Graph showing the maximum values of the cloud and non-cloud regions across spectral bands

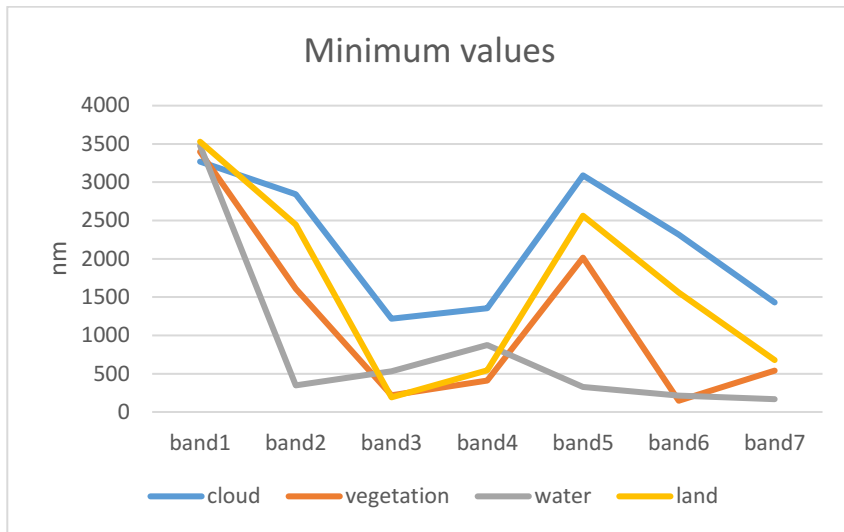


Figure 5-2. Graph showing the minimum values of the cloud and non-cloud regions across spectral bands:

Hence for the identification and separation of cloud across various spectral bands (band1-7) are shown with the help of graphs for cloud and non-cloud regions (vegetation, land, water) in Figures 5.1 and 5.2.

5.2 Manual masking method

The manual masking method is one of the methods used in the region of interest (ROI) technique. This method comprises of masking the cloud manually with the help of MATLAB. The masking of cloud is done by drawing the region of polygon by freehand to select the desired cloud part to be identified. The manual masking method is done to an extent until the image containing cloud obtained in this method matches to the automatic masked image containing cloud, which is discussed in coming chapter.

5.2.1 Freehand manual masking of cloud

The pictures of manually masked cloud vary according to the freehand selection of each image, as the cloud region of boundaries are marked with freehand.

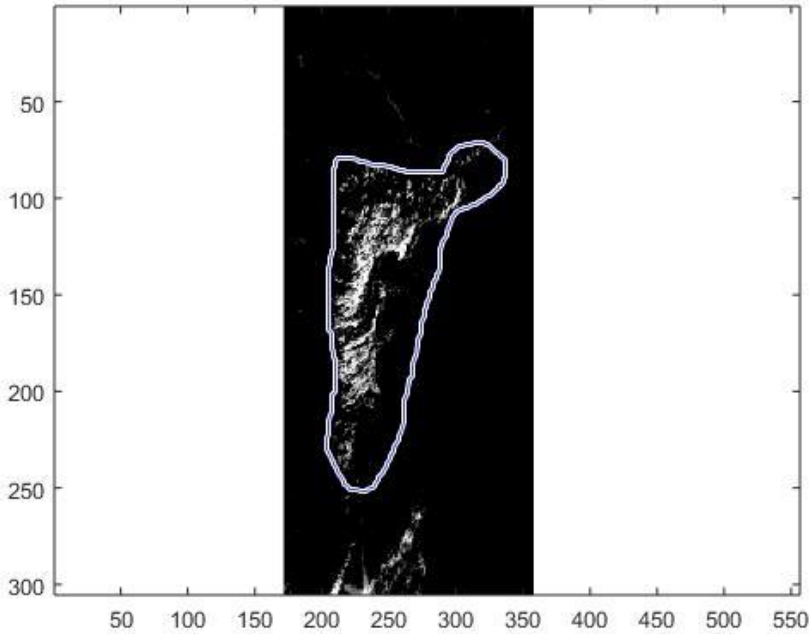


Figure 5-3. Freehand masking of cloud

Figure 5.3 shows the freehand masking of cloud depicted in the boundary.

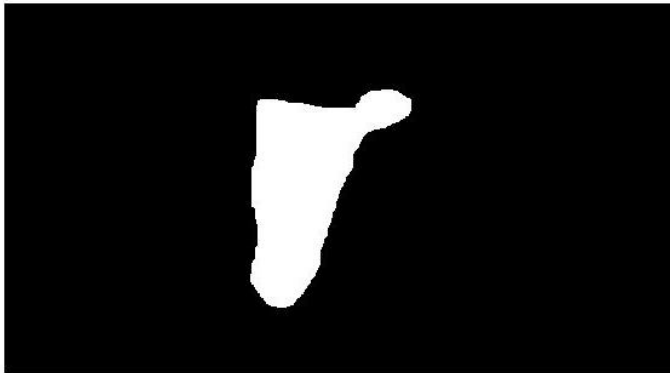


Figure 5-4. Masked patch of cloud

Figure 5.4 depicts the patch of cloud which is masked for the image shown in Figure 5.3.

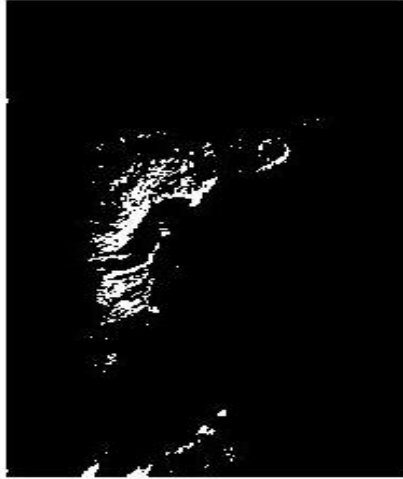


Figure 5-5. Actual cloud image

Figure 5.5 shows the desired or actual cloud image which is to be obtained.

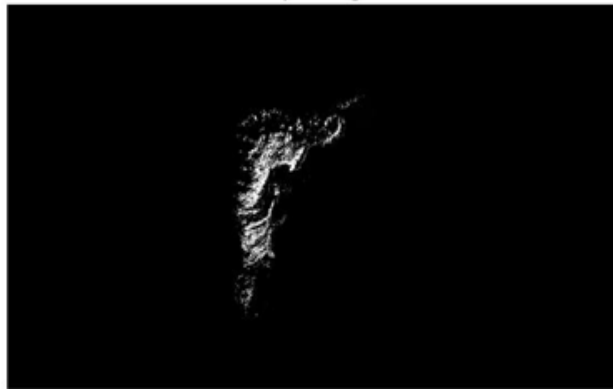


Figure 5-6. Image with cloud of the freehand masking method

Figure 5.6 shows the image of cloud obtained by the freehand masking method.

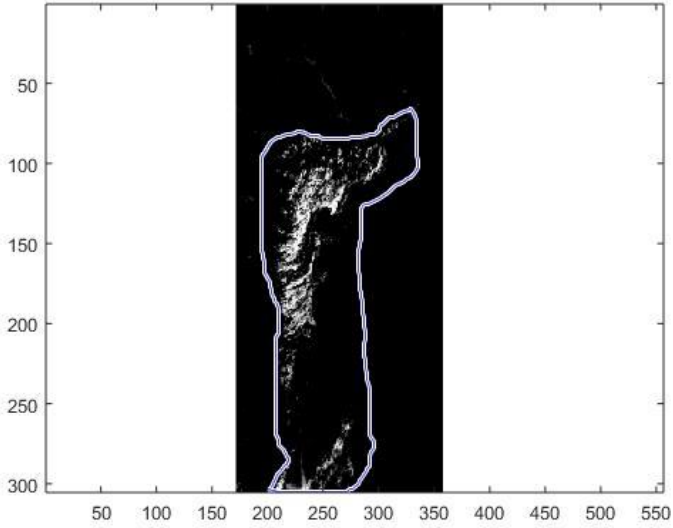


Figure 5-7. Freehand masking of cloud

Figure 5.7 depicts the freehand masking of cloud of different shape compared to Figure 5.3.

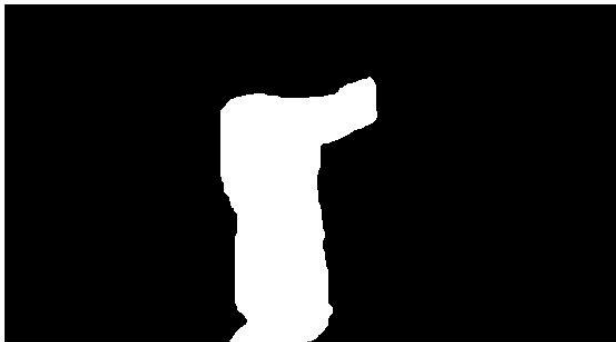


Figure 5-8. Masked patch of cloud

Figure 5.8 shows the masked patch of cloud which is masked for the image shown in Figure 5.7.



Figure 5-9. Image with cloud of the freehand masking method

Figure 5.9 depicts the image of cloud obtained by the freehand masking method with complete cloud, compared to Figure 5.6.

5.2.2 Manual masking of cloud by threshold varying

The manual masking of cloud is also obtained by manually varying the threshold until the cloud obtained by this method matched to the cloud obtained by freehand method. It is because the image intensity values are in the range $[0, 255]$. The images obtained by varying the threshold value are compared to the automatic masked cloud images to evaluate the performance of the automatic masking method. Here it is assumed that manually selected mask represent true cloud pixels in the image.

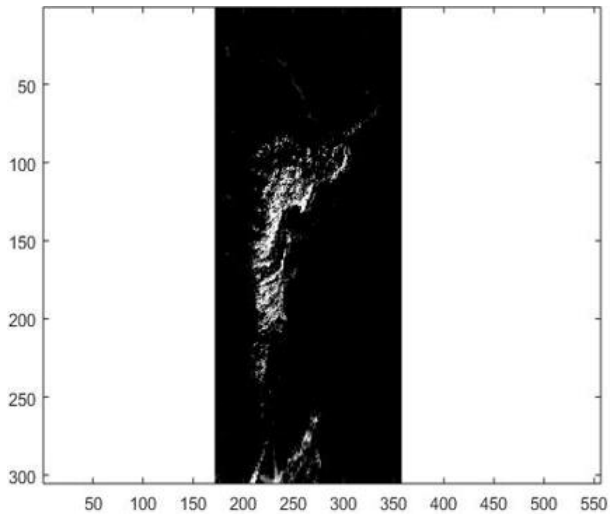


Figure 5-10. Original greyscale image

Figure 5.10 shows the original greyscale image on which the downsampling is done in order to apply the ROI selection technique.



Figure 5-11. Cloud image using manual masking method with threshold level=10

In Figure 5.11 the image shows a cloud which is obtained by manual masking method with threshold level is set to 10.

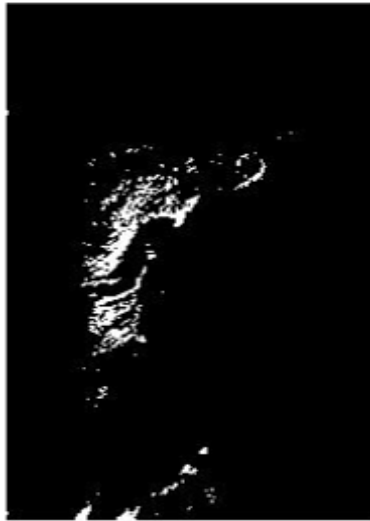


Figure 5-12. Cloud image using manual masking method with threshold level=129

Figure 5.12 depicts the cloud image obtained by setting the threshold level to 129 in the manual masking method.

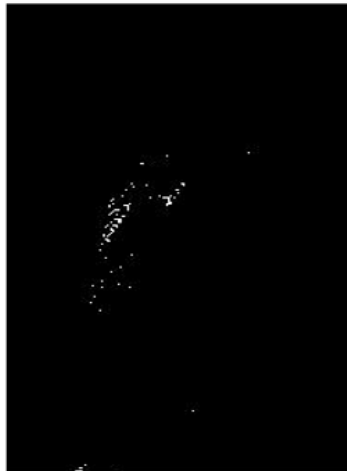


Figure 5-13. Cloud image using manual masking method with threshold level=250

By setting threshold level to 250 by manual masking, Figure 5.13 is obtained. The manually masked image using this optimal threshold will be compared to the images that are masked automatically.

5.3 Automatic masking method

The automatic method of masking is the other method in the region of interest (ROI) selection technique. The image obtained in this method is by automatic masking method. Here the threshold value is evaluated by using Otsu threshold method to 0.5059. The cloud image is then compared with the manual mask of cloud obtained by using optimal threshold $T=129$. Further the threshold level of the image in the automatic method should match the threshold level of cloud image obtained in the manual masking method. Hence the image containing the cloud obtained through automatic masking is further used to compare with the image of cloud obtained manual masked method.

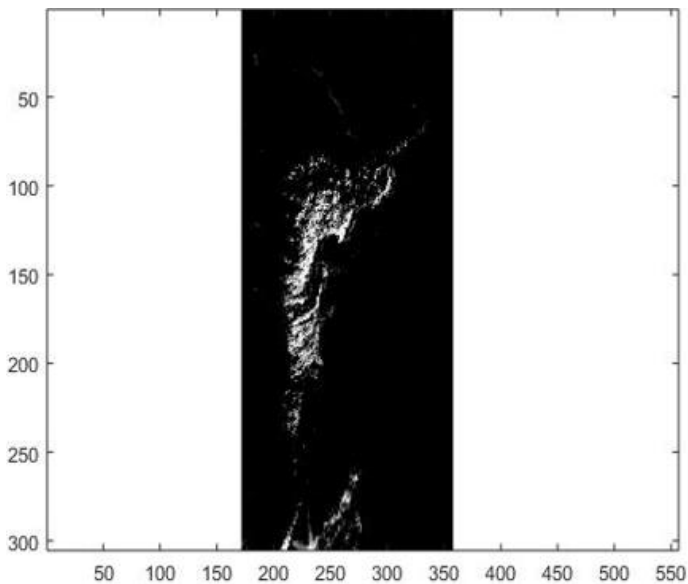


Figure 5-14. Original greyscale image

Figure 5.14 depicts the original greyscale image on which the downsampling is done in order to apply the ROI selection technique.

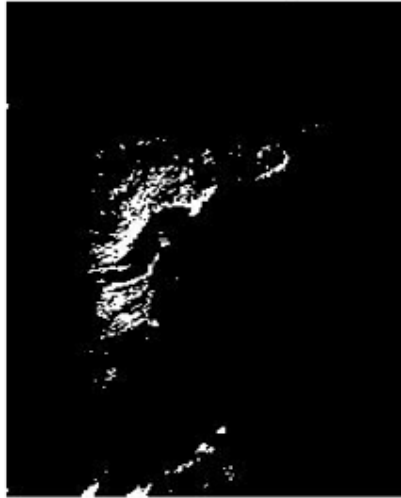


Figure 5-15. Cloud image using automatic masking method with threshold level=0.5059

In automatic masking method the threshold level set to 0.5059 by the algorithm which yields the image containing cloud shown in Figure 5.15.

5.4 Comparison and analysis of manual masking and automatic masking methods

The cloud images masked through the two masking methods i.e. manual masking by threshold varying and automatic masking methods are compared. On analysing both the cloud images, obtained in the manual and automatic methods, the following observations are made:

1. The cloud images obtained in both methods provided the manual mask threshold equal to 129 for the intensity values in the range of [0, 255], and the automatic threshold equal to 0.5059. This threshold 0.5059 for the intensity values in the range of [0, 1] corresponds to the threshold 129 for the intensity values in the range of [0, 255].
2. Both cloud images are based on the threshold values.
3. In both methods, the images containing cloud are considered as the most suitable for the respective test image when the threshold levels

are average values. i.e. in case of manual mask threshold is equal to 129, while in case of automatic mask the threshold is equal to 0.5059.

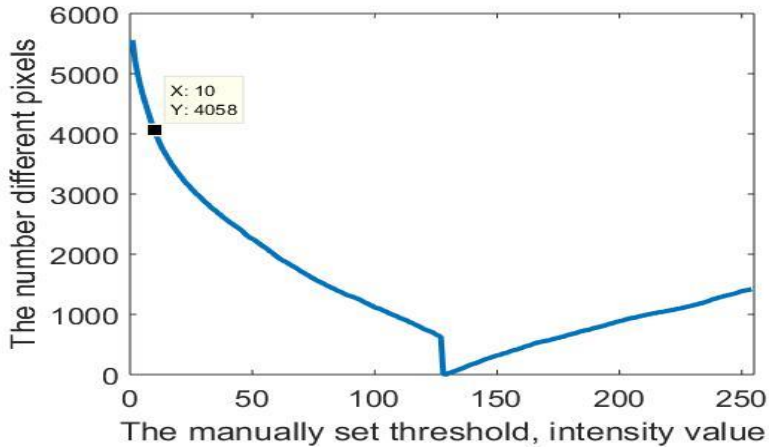


Figure 5-16. Graph showing manual threshold=10 and the pixel difference between automatic masking & manual masking=4058

Figure 5.16 shows a plot which depicts X=10 is the manually set threshold level in Y axis and k=4058 from equation 4.3 in chapter 4.6. which represents the number of different pixels between images acquired by using manual masking method and automatic masking method.

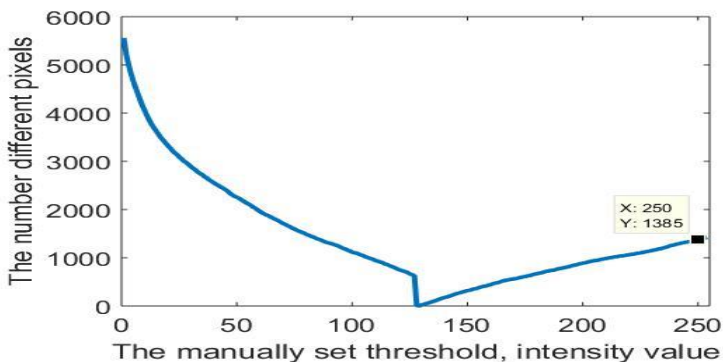


Figure 5-17. Graph showing manual threshold=250 and the pixel difference between automatic masking & manual masking=1385

Figure 5.17 shows that when manual threshold level=250 denoted by 'X' and with automatic threshold=0.5059 set by machine itself, the plot shows the difference between number of pixels $k=1385$ as 'Y' as shown in the plot.

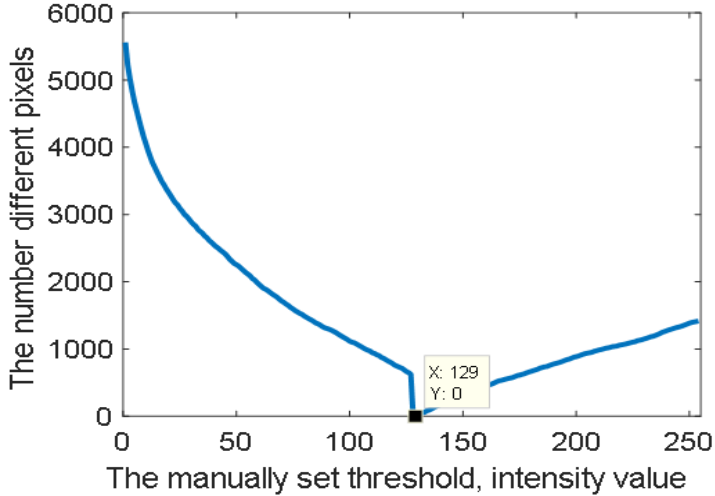


Figure 5-18. Graph showing manual threshold=129 and the pixel difference between automatic masking & manual masking=0

Figure 5.18 shows the plot when manual threshold level is set to 129 denoted by 'X' in the graph, and automatic threshold level=0.5059 set by the machine itself, then the difference between number of pixels of both manual and automatic masking methods is equal to zero shown by variable 'Y' in the plot.

5.5 Discussions

The images of the cloud acquired through the both methods i.e. manual masking by threshold varying method and automatic masking method are recognised as the desired cloud images. The ROI selection technique is used to obtain the images containing cloud from the original image. The TIFF image obtained from the QGIS is downsampled and the ROI selection technique is applied to the image. Further the image is converted to greyscale

image. The greyscale image is then considered as the original image. Now, the ROI selection technique is applied to the original image in order to identify the cloud and obtain the desired image. In the ROI selection technique there are two methods considered to be applied to the image. They are: manual masking method and automatic masking method. The manual masking method has two variations. They are: freehand manual masking and manual masking by varying threshold. In freehand masking the region of boundaries for the original image is drawn by freehand with the help of MATLAB. In the manual masking by threshold varying method, the level of threshold is varied until the desired image of cloud is obtained at that particular threshold value. Further the image acquired through manual masking method is compared with the automatic masking method. In the automatic masking method the machine itself sets the threshold value to a level, that allows to convert greyscale cloud image into its binary mask. In the automatic method the threshold level should be matched to the image containing cloud which is obtained in the manual masking method. The whole process of calculation of threshold levels are done with the help of MATLAB. Then, the cloud images of both the masking methods are compared and analysed such that they both yield the same desired cloud images. The comparison is done by applying manually set threshold $T=129$ for manual masking method and the automatically evaluated method threshold $T=0.5059$. With respect to these threshold values the equivalent cloud masks are obtained and it is confirmed by the zero difference obtained between the automatically and manually obtained cloud masks.

6 CONCLUSION AND FUTURE WORK

6.1 Conclusions

In this thesis, the cloud image obtained is by ROI selection technique. In this ROI selection technique the masking methods are done which comprises of manual and automatic methods. The manual part and automatic both yield the desired cloud images based on the threshold level. The manual method also contains freehand masking method to obtain the cloud image. The threshold levels of both the images are compared to acquire the desired image. In simple words, the quality of the desired image depends upon the threshold value. The threshold value is varied in manual masking to an extent until it yields the desired cloud image which is able to match with the cloud image obtained through automatic making method. Prior to this the original image which is used in the ROI technique is obtained through the MODIS sensor. The MODIS sensor produces images in HDF (Hierarchical Data Format) format image. Then this HDF image is converted into TIFF (tagged Image File Format) with the help of QGIS. QGIS helps to adjust the image quality by varying the contrast, brightness, and saturation of the image. Then this image is further modified with the help of MATLAB. Here in MATLAB the ROI technique is applied and the desired quality of cloud images are identified, obtained. This is done as the cloud in the actual image is considered to be as noise.

6.2 Future works

In this project many approaches, techniques, methods have been left for the future due to time constraint. The following ideas could be implemented:

1. To obtain the desired cloud and cloud free image, techniques other than ROI selection technique can be used such as Bag of words [24] and Support vector machine method (SVM) [25] and other methods by acquiring image from different sensors and satellites.
2. The images containing cloud can be acquired from the satellites of different variants.

3. The sensors of different types such as AWIFS-1, LISS-1, and others could be employed to obtain the images of the cloud and identify the images containing cloud.
4. Combination of sensors could also be a good idea in order to obtain the image including cloud.
5. The method can be further carried by filling the cloud area which is obtained, identified and considered as noise with the filling of segment with appropriate non-cloud areas like water, vegetation, land etc. which suits it better.

6.3 Challenges

Some sort of challenges were faced during the period of the thesis work. The major challenges were:

1. What is the methodology to be employed?
Methodology to be employed is a crucial step in obtaining the cloud image.
2. Learning or acquiring knowledge of QGIS software to read the data of the image.
Acquiring QGIS software knowledge is helpful in converting the HDF (Hierarchical Data Format) image to TIFF (Tagged image File Format) image.
3. What is the suitable sensor to be selected to obtain the suitable cloud image from the satellite?
Suitable sensor selection is necessary as various types of sensors are available and the best sensor which matches to the level of the thesis requirements is taken.
4. What are various techniques to be analyzed to identify the cloud?
Analyzing suitable technique like ROI selection technique is important to identify and mask the cloud.
5. Comparing and analyzing of the methods to generate the cloud images.
Comparison of images containing cloud obtained in both the methods is important step by comparing different threshold levels of manual masking and automatic masking methods.

References

- [1] T. M. Lillesand, R. W. Kiefer, and J. W. Chipman, *Remote sensing and image interpretation*, 5th ed. New York: Wiley, 2004.
- [2] A. M. Melesse, Q. Weng, P. S. Thenkabail, and G. B. Senay, “Remote Sensing Sensors and Applications in Environmental Resources Mapping and Modelling,” *Sensors*, vol. 7, no. 12, pp. 3209–3241, Dec. 2007.
- [3] “Fundamentals of Remote Sensing - George Joseph - Google Books.” [Online]. Available: https://books.google.co.in/books/about/Fundamentals_of_Remote_Sensing.html?id=peUFLCy4zLYC. [Accessed: 10-Sep-2018].
- [4] “IRS Satellites.” [Online]. Available: <http://uregina.ca/piwowarj/Satellites/IRS.html>. [Accessed: 10-Sep-2018].
- [5] “Landsat 8 | Landsat Missions.” [Online]. Available: <https://landsat.usgs.gov/landsat-8>. [Accessed: 18-Nov-2018].
- [6] “MODIS Web.” [Online]. Available: <https://modis.gsfc.nasa.gov/about/components.php>. [Accessed: 10-Sep-2018].
- [7] “IRS-1A.” [Online]. Available: <https://www.isac.gov.in/earth-observation/html/irs-1a.jsp>. [Accessed: 10-Sep-2018].
- [8] “MODIS Web.” [Online]. Available: <https://modis.gsfc.nasa.gov/>. [Accessed: 18-Nov-2018].
- [9] “Introducing GIS.” [Online]. Available: https://docs.qgis.org/testing/en/docs/gentle_gis_introduction/introducing_gis.html. [Accessed: 18-Nov-2018].
- [10] “Region of Interest (ROI) Tool.” [Online]. Available: <https://www.harrisgeospatial.com/docs/RegionOfInterestTool.html>. [Accessed: 18-Nov-2018].
- [11] “ROI-Based Processing - MATLAB & Simulink - MathWorks India.” [Online]. Available: <https://in.mathworks.com/help/images/roi-based-processing.html>. [Accessed: 01-Nov-2018].
- [12] C. Huang *et al.*, “Automated masking of cloud and cloud shadow for forest change analysis using Landsat images,” *Int. J. Remote Sens.*, vol. 31, no. 20, pp. 5449–5464, Oct. 2010.
- [13] D.-C. Tseng, H.-T. Tseng, and C.-L. Chien, “Automatic cloud removal from multi-temporal SPOT images,” *Appl. Math. Comput.*, vol. 205, no. 2, pp. 584–600, Nov. 2008.

- [14]L. Sun *et al.*, “A cloud detection algorithm-generating method for remote sensing data at visible to short-wave infrared wavelengths,” *ISPRS J. Photogramm. Remote Sens.*, vol. 124, pp. 70–88, Feb. 2017.
- [15]Y. Yuan and X. Hu, “Bag-of-Words and Object-Based Classification for Cloud Extraction From Satellite Imagery,” *IEEE J. Sel. Top. Appl. Earth Obs. Remote Sens.*, vol. 8, no. 8, pp. 4197–4205, Aug. 2015.
- [16]F. Liu, C. Li, and J. Yin, “Volcanic ash cloud extraction for RS image by combining PCA, ICA and SVM methods,” in *2016 IEEE Southwest Symposium on Image Analysis and Interpretation (SSIAI)*, 2016, pp. 153–156.
- [17]W. Kiadtikornthaweeyot, “Cloud cover automatic detection assessment for THAICHOTE satellite images,” in *2016 13th International Conference on Electrical Engineering/Electronics, Computer, Telecommunications and Information Technology (ECTI-CON)*, 2016, pp. 1–5.
- [18]B. Bat-Erdene, “Automatic region of interest determination method in dual energy X-ray absorptiometry of the femur and spine,” in *2016 11th International Forum on Strategic Technology (IFOST)*, 2016, pp. 263–266.
- [19]D. D. Rosa, C. Notarnicola, and F. Posa, “Cross-comparison and validation of MODIS AQUA cloud mask by using CLOUDSAT and CALIPSO datasets,” in *2009 IEEE International Geoscience and Remote Sensing Symposium*, 2009, vol. 3, pp. III-1019-III-1022.
- [20]L. Sun *et al.*, “A cloud detection algorithm-generating method for remote sensing data at visible to short-wave infrared wavelengths,” *ISPRS J. Photogramm. Remote Sens.*, vol. 124, pp. 70–88, Feb. 2017.
- [21]“The Remote Sensing Tutorial.” [Online]. Available: http://priede.bf.lu.lv/GIS/.Descriptions/RST/Sect16/nicktutor_16-7.shtml. [Accessed: 10-Sep-2018].
- [22]“File:Exploded View of MODIS Subsystems.gif - Wikimedia Commons.” [Online]. Available: https://commons.wikimedia.org/wiki/File:Exploded_View_of_MODIS_Subsystems.gif. [Accessed: 10-Sep-2018].
- [23]A. B. Patil, “OTSU Thresholding Method for Flower Image Segmentation,” p. 6.
- [24]Y. Zhang, R. Jin, and Z.-H. Zhou, “Understanding bag-of-words model: a statistical framework,” *Int. J. Mach. Learn. Cybern.*, vol. 1, no. 1, pp. 43–52, Dec. 2010.
- [25]S. Patel, “Chapter 2 : SVM (Support Vector Machine) — Theory,” *Machine Learning 101*, 03-May-2017.